Cs7Nd11(SeO3)12Cl16 : First Noncentrosymmetric Structure among Alkaline-Metal Lanthanide Selenite Halides

8 AUTHORS, INCLUDING:

Peter S Berdonosov
Lomonosov Moscow State University
69 PUBLICATIONS   **519** CITATIONS

SEE PROFILE

Philippe Smet
Ghent University
124 PUBLICATIONS   **2,028** CITATIONS

SEE PROFILE

Dirk Poelman
Ghent University
198 PUBLICATIONS   **3,253** CITATIONS

SEE PROFILE

Cs$_7$Nd$_{11}$(SeO$_3$)$_{12}$Cl$_{16}$: First Noncentrosymmetric Structure among Alkaline-Metal Lanthanide Selenite Halides

Peter S. Berdonosov,[*,†] Lev Akselrud,[‡] Yurii Prots,[‡] Artem M. Abakumov,[§] Philippe F. Smet,[⊥] Dirk Poelman,[⊥] Gustaaf. Van Tendeloo,[§] and Valery A. Dolgikh[†]

[†]Department of Chemistry, Moscow State University, Leninskie Gory 1 build, 3 GSP-1, 119991 Moscow, Russia
[‡]Max-Planck-Institut für Chemische Physik fester Stoffe, Nothnitzer Strasse 40, Dresden 01187, Germany
[§]EMAT, University of Antwerp, Groenenborgerlaan 171, B-2020 Antwerp, Belgium
[⊥]LumiLab, Department of Solid State Sciences, Ghent University, Krijgslaan 281-S1, 9000 Gent, Belgium

Ⓢ Supporting Information

ABSTRACT: Cs$_7$Nd$_{11}$(SeO$_3$)$_{12}$Cl$_{16}$, the complex selenite chloride of cesium and neodymium, was synthesized in the NdOCl−SeO$_2$−CsCl system. The compound has been characterized using single-crystal X-ray diffraction, electron diffraction, transmission electron microscopy, luminescence spectroscopy, and second-harmonic-generation techniques. Cs$_7$Nd$_{11}$(SeO$_3$)$_{12}$Cl$_{16}$ crystallizes in an orthorhombic unit cell with a = 15.911(1) Å, b = 15.951(1) Å, and c = 25.860(1) Å and a noncentrosymmetric space group $Pna2_1$ (No. 33). The crystal structure of Cs$_7$Nd$_{11}$(SeO$_3$)$_{12}$Cl$_{16}$ can be represented as a stacking of Nd$_{11}$(SeO$_3$)$_{12}$ lamellas and CsCl-like layers. Because of the layered nature of the Cs$_7$Nd$_{11}$(SeO$_3$)$_{12}$Cl$_{16}$ structure, it features numerous planar defects originating from occasionally missing the CsCl-like layer and violating the perfect stacking of the Nd$_{11}$(SeO$_3$)$_{12}$ lamellas. Cs$_7$Nd$_{11}$(SeO$_3$)$_{12}$Cl$_{16}$ represents the first example of a noncentrosymmetric structure among alkaline-metal lanthanide selenite halides. Cs$_7$Nd$_{11}$(SeO$_3$)$_{12}$Cl$_{16}$ demonstrates luminescence emission in the near-IR region with reduced efficiency due to a high concentration of Nd^{3+} ions causing nonradiative cross-relaxation.
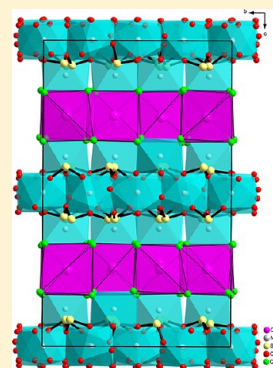
1. INTRODUCTION

During the past decade, mixed-anion compounds of lanthanides exhibit a sustained growth of scientific interest because of their rich crystal chemistry and interesting physical properties suitable for practical utilization.[1] The group of selenite halides of bismuth or lanthanides (Ln) contains the selenium atoms in oxidation state 4+, demonstrating a highly stereochemically active lone electron pair. Because of the strongly asymmetric surroundings of selenium, the selenite groups together with halide atoms tend to act as terminal groups playing the role of structural spacers. A combination of the selenite groups and halide ions in the crystal structure makes this family very attractive in the search for open-framework structures, low-dimensional structures, pyro-, piezo-, or ferroelectric materials, and/or nonlinear optical materials.[2−6]

Recently, successful preparations of the mixed-anion selenite halides of lanthanides and alkaline metals have been reported.[7−15] One can expect that these compounds could form a relatively large family because of their ability to combine different structural blocks, such as (Ln$_{11}$(SeO$_3$)$_{12}$, CsCl-like blocks, and layers of halide atoms, as demonstrated by the selected examples of the CsSm$_{21}$(SeO$_3$)$_{24}$Br$_{16}$,[7] Rb$_6$LiLn$_{11}$(SeO$_3$)$_{12}$Cl$_{16}$ (Ln = Pr, Nd),[9,13] and Cs$_3$La$_{11}$(SeO$_3$)$_{12}$Cl$_{12}$ structures.[15] All rare-earth selenite halides known so far are centrosymmetric. As follows from the valence-matching principle,[16] the mixed selenite halides demonstrate a trend toward different anion surroundings for the metal ions

M$^+$, Ln^{3+}, and Se^{4+} with different Lewis acidity. In the extreme case, it could lead to so-called salt-inclusion solids (SIS) compounds,[17,18] which are promising candidates for non-centrosymmetric (NC) structures. Revelation of the structural peculiarities and their correlation with the chemical composition for this group of compounds requires experimental data on the mixed-anion selenite halides of lanthanide and alkaline metals.

In the present study, we report the synthesis and crystal structure of a new selenite chloride of neodymium and cesium with the composition Cs$_7$Nd$_{11}$(SeO$_3$)$_{12}$Cl$_{16}$. This compound extends the M$_x$Ln$_{11}$(SeO$_3$)$_{12}$Hal$_{x+9}$ (M = alkaline metal; Ln = La, Pr, Nd, Sm; Hal = Cl, Br) family[7,9,13−15] and demonstrates a NC structure. As far as we know, this is the first example of a NC structure among the M$_x$Ln$_{11}$(SeO$_3$)$_{12}$Cl$_y$ compounds.

2. MATERIALS AND METHODS

2.1. Synthesis. Cs$_7$Nd$_{11}$(SeO$_3$)$_{12}$Cl$_{16}$ crystals were synthesized by reaction in an evacuated sealed quartz tube. The initial materials NdOCl and SeO$_2$ were obtained by the techniques described elsewhere.[6] NdOCl (0.275 g, 1.41 mmol) and anhydrous SeO$_2$ (0.158 g, 1.42 mmol) were taken in a 1:1 molar ratio. They were mixed with CsCl (0.860 g, 5.11 mmol), whose weight was twice the mass of the NdOCl−SeO$_2$ mixture. The total sample weight was ~1.3 g. The sample preparation was performed in an argon-filled chamber.

The mixture was loaded into evacuated and sealed silica tubes and preheated for 24 h at 300 °C, and then the temperature was raised up to 660 °C. The sample was exposed at this temperature for 15 min, then cooled at 2 K/h to 400 °C, and then furnace-cooled to room temperature. The obtained pink cake was washed with distilled water and ethanol to remove excess CsCl. The final substance, consisting of pink platelike crystals, was dried in air. The yield of the resulting substance was 0.430 g (~80% relative to loaded SeO_2).

2.2. Composition and Structure Determination. The composition of seven randomly selected crystals with different shapes was examined with energy-dispersive X-ray (EDX) analysis using a JEOL JSM6490LV scanning electron microscope equipped with a Si(Li) detector (INCAx-Sight Oxford Instruments). EDX spectra from three to four points of each crystal revealed very similar Cs:Nd:Se ratios for all investigated crystals. The average composition was found to be Cs 24.1 ± 3, Nd 36.9 ± 3, and Se 38.9 ± 3 atomic %.

Testing the crystals on a Rigaku AFC7 diffractometer equipped with a Saturn 724+ CCD detector revealed an orthorhombic unit cell with lattice parameters $a \sim b \sim 15.9$ Å and $c \sim 25.8$ Å. Structure solution with direct methods and structure refinement were performed with *WinCSD* software.[19] The solution was obtained in an orthorhombic unit cell with $a = 15.911(1)$ Å, $b = 15.951(1)$ Å, and $c = 25.860(1)$ Å, and the structure was refined in the NC space group $Pna2_1$ (No. 33) (see Table 1 for details). Atomic coordinates and atomic displacement

Table 1. Crystallographic Data for $Cs_7Nd_{11}(SeO_3)_{12}Cl_{16}$

space group	$Pna2_1$
cell constants (Å)	
a	15.911(1)
b	15.951(1)
c	25.860(1)
cell volume (Å³)	6563.2(9)
calcd density (g/cm³)	4.6628(8)
abs coeff (cm⁻¹)	203.23
radiation and wavelength, λ, Å	Mo Kα, 0.71073
mode of refinement	$F(hkl)$
restrictions	$F(hkl) > 4.00\sigma(F)$
weighing scheme	varying $1/\ln[F(\text{obs}) \times 4]$
no. of atom sites	82
2Θ and $\sin\Theta/\lambda$(max)	65.18 and 0.758
no. of measd reflns	29001
no. of unique reflns	16748
$R(\sigma)$, $R(\text{eq})$	0.082, 0.052
$R(F)$, R_w	0.0460, 0.0477
GOF	1.020
software used for refinement	*WinCSD*19

parameters are listed in Table S1 in the Supporting Information (SI). The list of interatomic distances for the $Cs_7Nd_{11}(SeO_3)_{12}Cl_{16}$ crystal structure is provided in Table S2 in the SI. The $Cs_7Nd_{11}(SeO_3)_{12}Cl_{16}$ formula derived from the structure analysis is in a good agreement with the EDX results.

In order to confirm an absence of the inversion center in the $Cs_7Nd_{11}(SeO_3)_{12}Cl_{16}$ structure, an experiment was performed using second harmonic generation (SHG) of a laser beam by a powder technique, with a setup similar to that employed by Kurtz and Perry.[20] An YAG:Nd laser was used as a source of powerful pulsed radiation at a wavelength $\lambda = 1.064$ μm with a repetition rate of 4 Hz and a pulse duration of about 10 ns. The intensity $I_{2\omega}$ of the signal at doubled frequency ($\lambda = 0.532$ μm) was registered in the backward direction. The measured signal obtained from a ground powder of the raw reaction mixture in relation to the SHG intensity of α-quartz powder with the same particle size was about 1. This confirms the NC structure solution.

2.3. Transmission Electron Microscopy (TEM) Study. TEM specimens were prepared by dispersing $Cs_7Nd_{11}(SeO_3)_{12}Cl_{16}$ in ethanol and depositing drops of the suspension on a holey carbon

grid. Electron diffraction (ED) and high-resolution transmission electron microscopy (HRTEM) images were obtained with a FEI Tecnai G² microscope operated at 200 kV. The compound is extremely sensitive to electron-beam irradiation. Therefore, all operations were performed with a drastically reduced intensity of the electron beam, but even then gradual amorphization occurs. HRTEM images were taken at low-dose conditions, resulting in a rather poor signal-to-noise ratio.

2.4. Luminescence Study. Luminescence spectra were recorded on a FS920 steady-state fluorescence spectrometer (Edinburgh Instruments) using a 450 W xenon light source and a double-excitation monochromator. Emission spectra were acquired in scanning mode with a liquid-nitrogen-cooled germanium IR detector (wavelength range 800−1650 nm). All emission and excitation spectra were corrected for the instrument response. Measurements were performed at 75 K, using an Optistat CF cryostat (Oxford Instruments).

3. RESULTS AND DISCUSSION

The sample obtained after the spontaneous crystallization process in the NdOCl−CsCl−SeO₂ system contains the
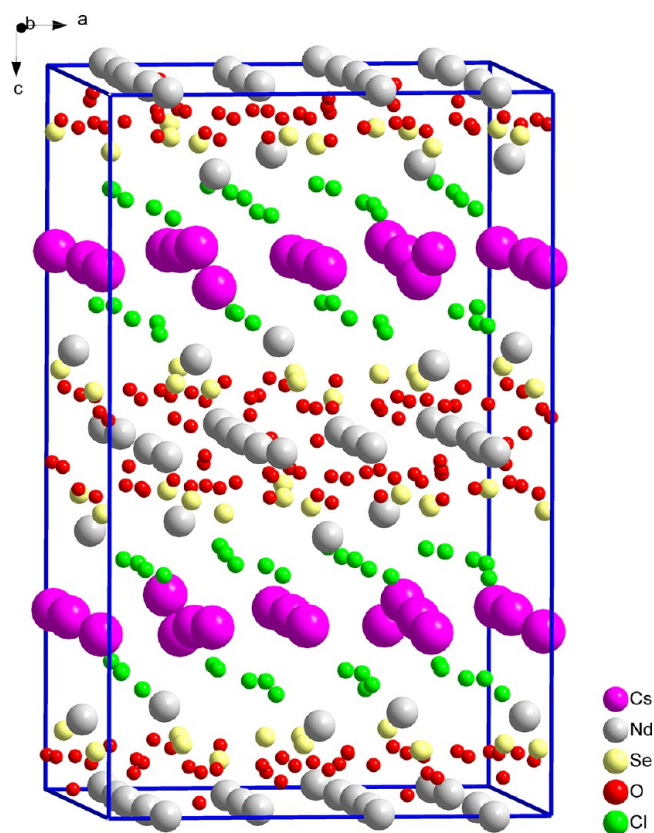

Figure 1. Unit cell of $Cs_7Nd_{11}(SeO_3)_{12}Cl_{16}$.

$Cs_7Nd_{11}(SeO_3)_{12}Cl_{16}$ phase as the main constituent. The crystal structure was established by means of single-crystal X-ray diffraction (Tables 1 and S1 and S2 in the SI) and examined by TEM. The chemical composition $Cs_7Nd_{11}(SeO_3)_{12}Cl_{16}$ was established by the structural refinement and confirmed by EDX analysis. The NC character of the structure was confirmed by the SHG measurement.

Occasionally, single crystals were found with a set of reflections pointing at a doubling of the unit cell along the c axis ($c \approx 51.6$ Å). We did not succeed in solving the crystal structure of this compound because of the poor quality of the
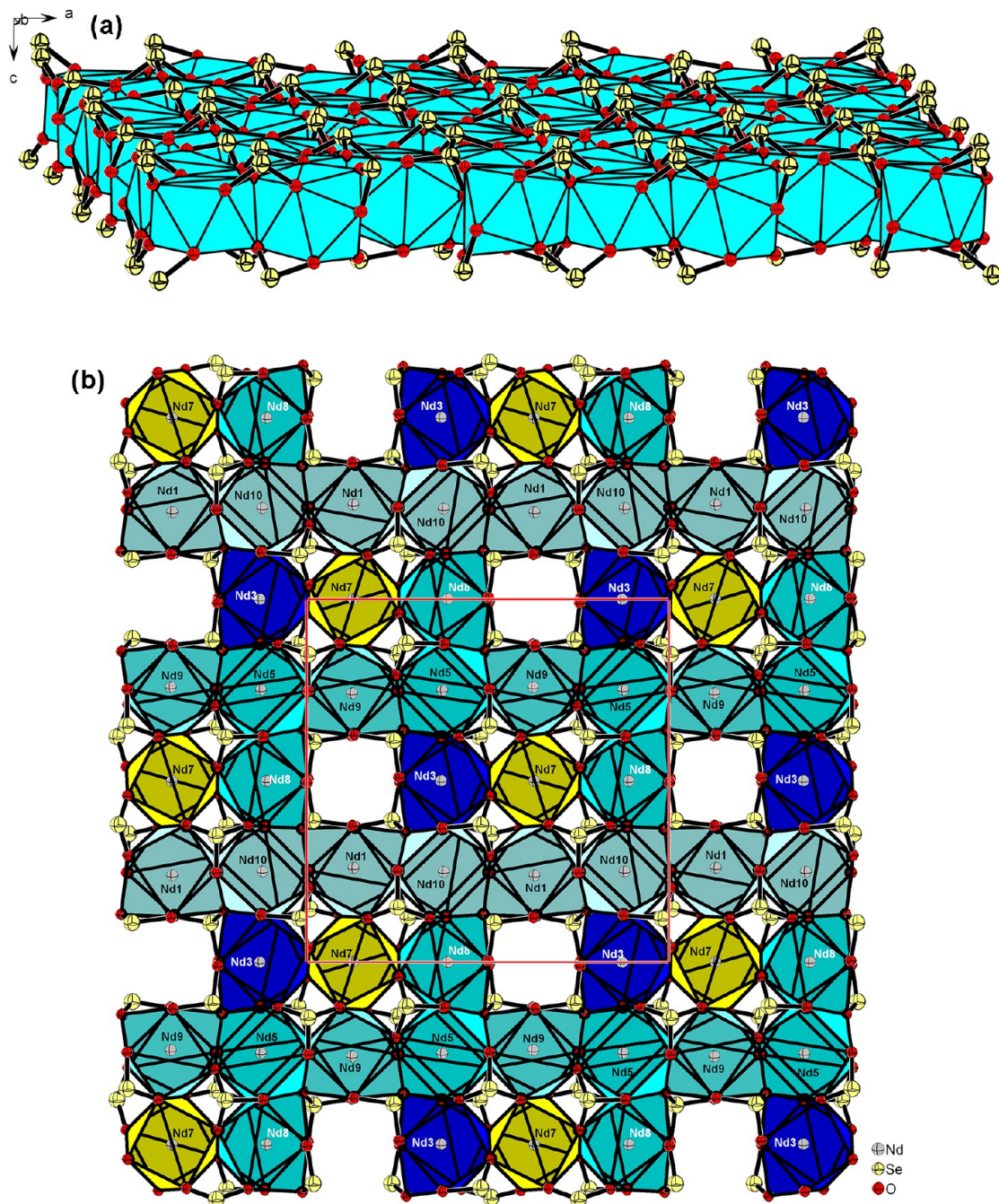
Figure 2. (a) Layer constructed from the $[NdO_{10}]$ polyhedra. The unit cell is outlined. (b) SeO_3 groups acting as additional stitching.

single crystals. Detailed analysis of this admixture phase is beyond the scope of this paper.

The content of the unit cell of the $Cs_7Nd_{11}(SeO_3)_{12}Cl_{16}$ structure is shown in Figure 1. It contains 11 independent neodymium atoms. Seven neodymium atoms (Nd1, Nd3, Nd5, Nd7, Nd8, Nd9, and Nd10) have a coordination environment formed exclusively by oxygen atoms. Four neodymium atoms (Nd2, Nd4, Nd6, and Nd11) are coordinated by oxygen and chlorine atoms (Table S2 in the SI). The Nd7 atom has a square-antiprismatic $[Nd7O_8]$ oxygen coordination. The Nd1, Nd3, Nd5, Nd8, Nd9, and Nd10 atoms are situated in 10-vertex oxygen polyhedra. Originally, such unusually high coordination numbers for the Ln^{3+} ions were observed only in selenates(IV) $NaLn(SeO_3)_2$ (Ln = La, Y).[21] In the case of the M–Ln selenite

halides (M = Cs, Rb; Ln = Sm, Pr, Nd) a coordination number 10 for the Ln^{3+} ions is usually observed.[7,10,14]

All of the O–Cl mixed neodymium polyhedra have distorted square-antiprismatic $[NdO_4Cl_4]$ geometry with one base constructed of oxygen ions and another base made of chloride ions. The Nd–O distances (d(Nd–O) = 2.36–2.85 Å in the $[Nd7O_8]$ polyhedra and 2.31–2.52 Å in the $[NdO_4Cl_4]$ polyhedra) and the Nd–Cl distances (2.81–3.08 Å) are in a good agreement with the interatomic distances in the related neodymium-based compounds. For example, in $NdSeO_3Cl$, the Nd–O bond lengths are in the range of 2.38–2.86 Å and the Nd–Cl bond lengths are in the range of 2.79–3.04 Å.[4]

The 10-vertex $[Nd9O_{10}]$ and $[Nd5O_{10}]$ polyhedra share triangular faces and form chains along the [100] direction. Similar chains are built by the $[Nd1O_{10}]$ and $[Nd10O_{10}]$

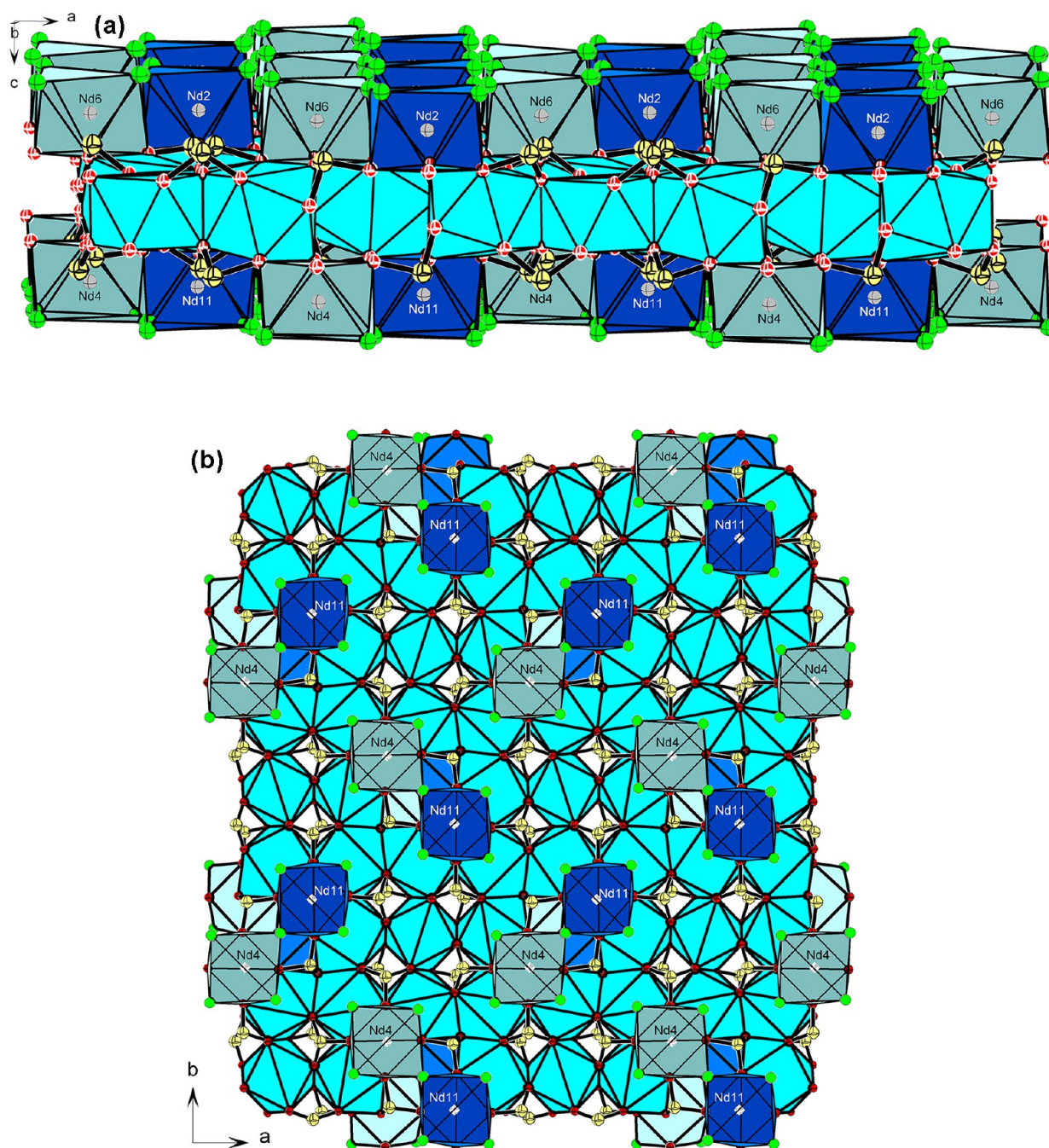**Figure 3.** Nd−Se−O−Cl layers: (a) side view; (b) top view. [NdO$_4$Cl$_4$] antiprisms are drawn lighter and darker.

polyhedra (Figure 2a). Each pair of [Nd1O$_{10}$] and [Nd9O$_{10}$] polyhedra is connected by the [Nd7O$_{10}$] polyhedron along the [010] direction through edge-sharing (Figure 2a). The [Nd10O$_{10}$] and [Nd5O$_{10}$] polyhedra belonging to different chains are connected by common triangular faces, with the [Nd3O$_{10}$] or [Nd8O$_{10}$] polyhedra along [010]. As a result, the 10-fold polyhedra form (001) layers. These layers contain chessboard-ordered large voids (vacant neodymium positions) of about 4 Å diameter (Figure 2a) and smaller voids (with diameters of about 2.6−2.7 Å), which are situated around the [Nd7O$_{10}$] polyhedra. If the large voids would be occupied by the neodymium atoms, a net with ∼4 × 4 Å square meshes in the *ab* plane would occur. However, an ordered arrangement of the voids requires a larger ∼16 × 16 Å metric of the unit cell.

The selenium atoms are situated on both sides of the Nd−O layer. All of them are concentrated near the voids in the Nd−O layer, being connected with three oxygen atoms from the [NdO$_{10}$] polyhedra (Figure 2a,b). The SeO$_3$ groups feature a pyramidal shape SeO$_3$E, which is usual for Se^{IV}, where E is a lone electron pair. Most of the Se−O distances are in the range of 1.66−1.75 Å with the only exclusions the Se3−O7, Se5−O27, and Se6−O5 distances (Table S2 in the SI). We believe that these either shorter or longer distances reflect imperfections of the examined crystal and/or disorder in the structure stacking, as observed by TEM (see below). The SeO$_3$E groups serve as an additional stitching for the Nd−O layer.

Above and below the Nd−O layer are located the Nd2, Nd4 and Nd6, Nd11 atoms. All of them are coordinated by four
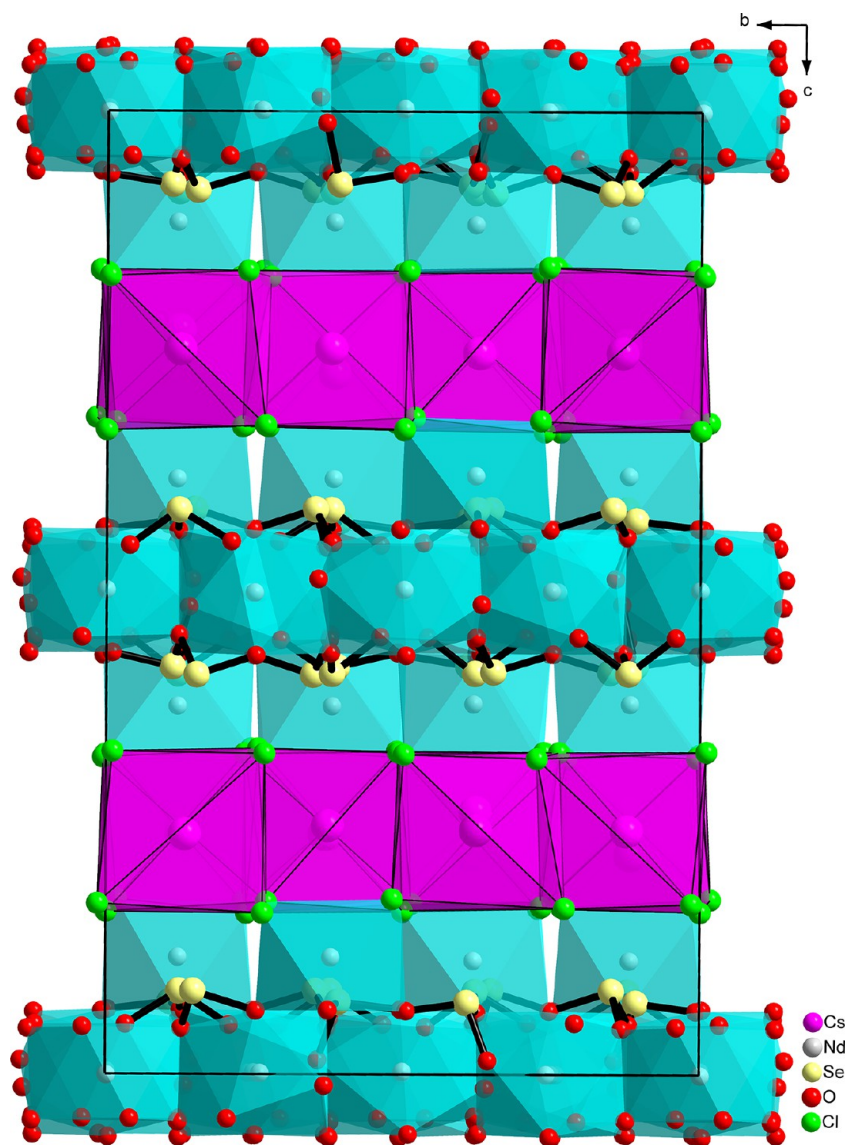
Figure 4. Polyhedral representation of the $Cs_7Nd_{11}(SeO_3)_{12}Cl_{16}$ crystal structure along the $[100]$ direction.

oxygen atoms from the Nd−O layer from one side and four chloride ions from the other side, forming square antiprisms. These antiprisms are connected pairwise by a common chloride vertex and situated above and below the large voids of the Nd−O layer (Figure 3). The layers of chlorine atoms are separated by the cesium atomic layers. All cesium atoms are coordinated in cubelike polyhedra by chloride anions from the $[NdO_4Cl_4]$ antiprisms of the Nd2, Nd4 or Nd6, Nd11 atoms. Only the Cl10 atom is not engaged in the $[NdO_4Cl_4]$ antiprisms and belongs solely to the $[CsCl_8]$ cubes.

As a result, the $Cs_7Nd_{11}(SeO_3)_{12}Cl_{16}$ structure can be considered as a stacking of CsCl-type Cs_7Cl_{16} lamellas and $Nd_{11}(SeO_3)_{12}$ lamellas, being linked through layers of chlorine ions. The interatomic distances within the Nd−Se−O blocks and the CsCl-like blocks are significantly different, allowing us to consider $Cs_7Nd_{11}(SeO_3)_{12}Cl_{16}$ as a SIS compound[17,18] (Figure 4).

Taking into account the layered nature of the $Cs_7Nd_{11}(SeO_3)_{12}Cl_{16}$ structure, we have performed TEM investigations to reveal possible violations in the stacking of the Cs_7Cl_{16} and $Nd_{11}(SeO_3)_{12}$ lamellas. Typical ED patterns are

shown in Figure 5. The $[001]$ and $[010]$ ED patterns can be indexed within an orthorhombic primitive unit cell with the lattice parameters $a \approx b \approx 15.9$ Å and $c \approx 25.9$ Å, in agreement with the unit cell used for the crystal structure determination. The $h0l$, $h = 2n$, reflection condition is clearly observed in the $[010]$ ED pattern, in agreement with the space group $Pna2_1$. The $hk0$, $h + k \neq 2n$, reflections in the $[001]$ ED pattern are very weak and barely observed. This reflects that the structure does not depart far from the centrosymmetric space group $Pnan$ because of rather small atomic displacements, leading to the acentric $Pna2_1$ structure.

No signs of disorder or planar defects were found when the structure is viewed along the $[001]$ and $[010]$ axes. However, the $[1\bar{1}0]$ ED pattern demonstrates pronounced diffuse intensity along c^*; extra spots in the $[hh0]$, $h = 4n$, rows, and displacements of the spots in the $[hh0]$, $h \neq 4n$, rows. The latter are different for different crystallites; two typical examples are given in Figure 5.

The $[1\bar{1}0]$ HRTEM image in Figure 6 shows stacking faults in the structure. Although the signal-to-noise ratio is low because of the low stability of the compound under electron
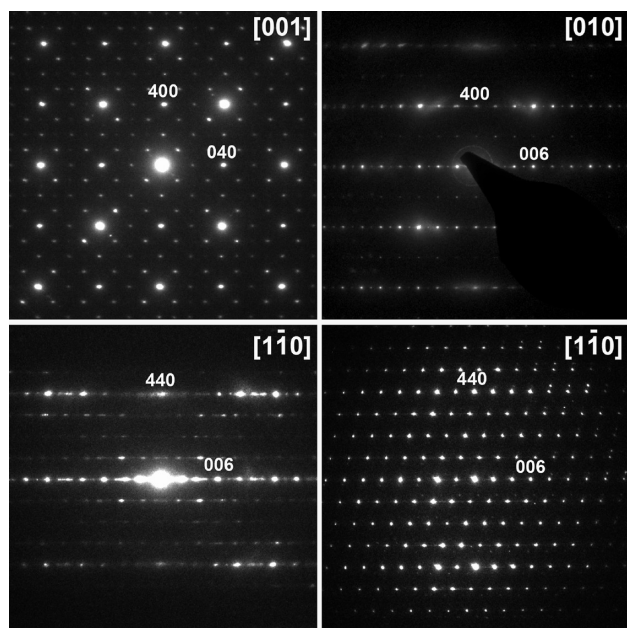
Figure 5. ED patterns of $Cs_7Nd_{11}(SeO_3)_{12}Cl_{16}$.

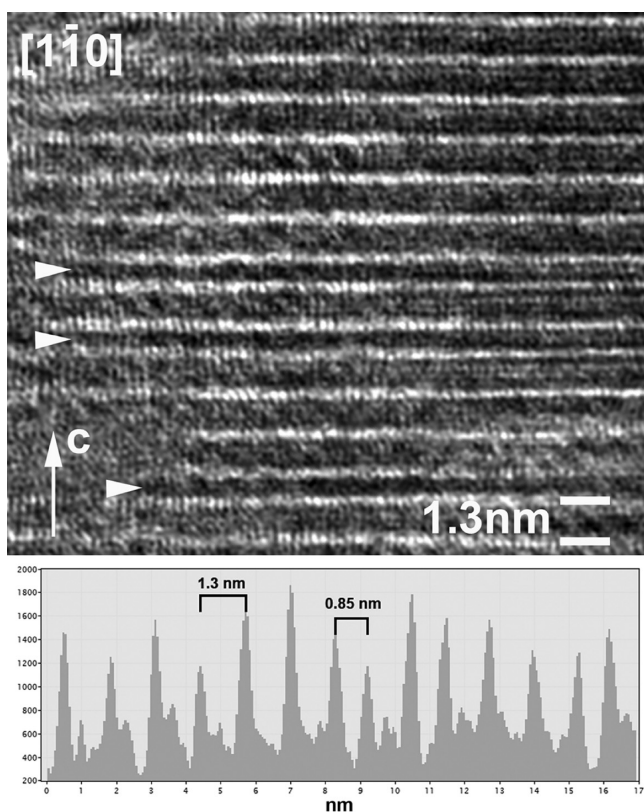**Figure 6.** $[1\bar{1}0]$ HRTEM image showing violation of the perfect layer stacking sequence with a ~13 Å distance between the $Nd_{11}(SeO_3)_{12}$ lamellas (brightest rows) by the occurrence of thinner ~8.5 Å lamellas marked with arrowheads. The intensity profile across the layer demonstrating variation of the interlayer separations is shown below.

irradiation, which does not allow unambiguous assignment of the atomic layers, one can speculate, based on measurements of the interlayer distances, that the brighter layers correspond to the median layer of the $Nd_{11}(SeO_3)_{12}$ lamellas in the structure. The distance between these layers is equal to ~13 Å (=1/2c).

The perfect sequence of the layers is violated by the blocks, where these median layers are separated by ~8.5 Å only (marked by arrowheads in Figure 6, top). The difference in spacing between the layers is obvious from the intensity profile across the layers shown in Figure 6b. Shrinkage of the interlayer distance from ~13 to ~8.5 Å corresponds well to the subtraction of one CsCl-type lamella with a thickness of ~4.3 Å. The obtained block configuration (Figure 7) contains two $Nd_{11}(SeO_3)_{12}$ lamellas linked together by a layer of chlorine atoms. Similar blocks compose the crystal structure of the $(Cs,Sm)_{11}(SeO_3)_{12}Br_8$ compound.[7] This type of stacking fault can be associated with the extra reflections in the $[hh0]$, $h = 4n$, rows (see the $[1\bar{1}0]$ zone in Figure 6) because these stacking faults change the average periodicity along the c axis. The displacement of the spots in the $[hh0]$, $h \neq 4n$, rows is associated with shifts of the $Nd_{11}(SeO_3)_{12}$ lamellas in the ab plane. Looking at the $[1\bar{1}0]$ structure projection, one can expect a possibility for lateral displacement of the lamellas by a $\pm n/8[110]$ projected vector (actual shifts can be, for example, $\pm 1/4[100]$ or $\pm 1/4[010]$). Alternation of the lamellas with different displacement vectors can be ordered, locally resulting in a diffuse intensity and changing positions of the $[hh0]$, $h \neq 4n$, reflections arising from the ordering in these lamellas. Two possibilities are schematically illustrated in Figure 8. Alternating displacements by $1/8[110]$ and $-1/8[110]$ projected vectors result in an orthorhombic structure (as refined from XRD data, bottom left ED pattern in Figure 5), whereas cumulative displacements by a $1/8[110]$ projected vector result in a monoclinic structure (bottom right ED pattern in Figure 5). HRTEM images in Figure 9 demonstrate that displacements over $1/4[110]$ are also possible, locally resulting in another polytype.

Pseudosymmetry of the $Cs_7Nd_{11}(SeO_3)_{12}Cl_{16}$ structure was analyzed using the *PSEUDO* program of the Bilbao crystallographic server.[22] (the SI file contains the routine output). As expected from the very low intensity of the $hk0$, $h + k \neq 2n$, reflections and weak SGS signal, the structure is very close to its centrosymmetric counterpart with the space group *Pnan*. Cesium, neodymium, and selenium atoms demonstrate only negligible shifts from the centrosymmetric positions (<0.1 Å). The largest acentric displacements are associated with the atomic pairs O26−O27 (0.19 Å), Cl6−Cl15 (0.16 Å), and Cl8−Cl13 (0.24 Å).

The $Cs_7Nd_{11}(SeO_3)_{12}Cl_{16}$ compound is the third member of a family with the general composition $M_7Ln_{11}(SeO_3)_{12}Cl_{16}$ (M = alkaline metal; Ln = Pr, Nd, Sm) and an extended family with the composition $M_xLn_{11}(SeO_3)_{12}Cl_y$ (Table 2). All of these structures are constructed in the same manner: the lanthanide−oxide−chloride-layered blocks are additionally stitched by the SeO_3E selenite groups and separated by the CsCl-like blocks. The common feature of these phases is the pseudotetragonal ~16 × 16 Å unit cell mesh in the ab plane. This fact can be explained by a similar structure of the central Ln−O layer, where the lanthanide atoms sit at the nodes of a ~4 × 4 Å square mesh and the increase of the cell dimensions in the ab plane is caused by ordering of the lanthanide atoms and vacancies. In spite of striking similarity between these structures, $Cs_7Nd_{11}(SeO_3)_{12}Cl_{16}$ is not isostructural to other compounds and represents the first example of a non-centrosymmetric structure in this family. As a main difference between $Cs_7Nd_{11}(SeO_3)_{12}Cl_{16}$ and K−Sm or Cs−Pr selenite chlorides $M_7Ln_{11}(SeO_3)_{12}Cl_{16}$,[14] the ordered arrangement of the lanthanide atoms and vacancies in the $[LnO_4Cl_4]$

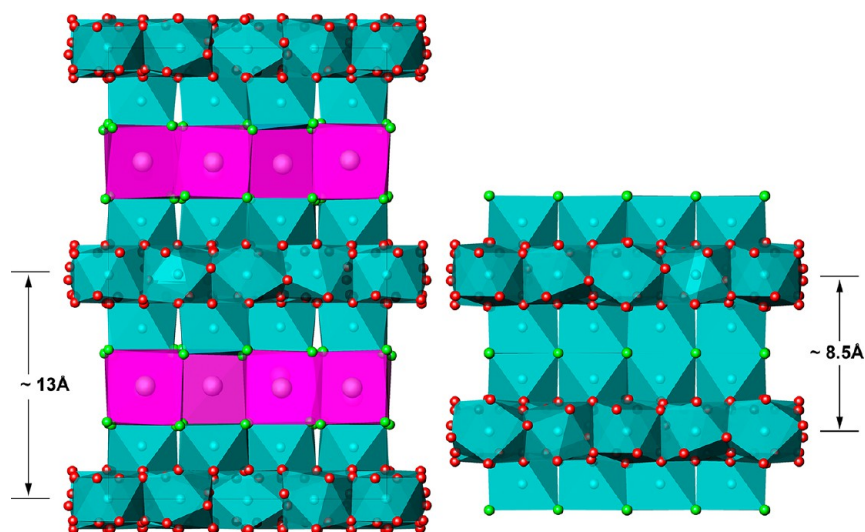**Figure 7.** $Cs_7Nd_{11}(SeO_3)_{12}Cl_{16}$ structure viewed along the $[1\bar{1}0]$ direction (left). Selenium and oxygen atoms are not shown. The ~8.5 Å $(Cs,Sm)_{11}(SeO_3)_{12}Br_8$-type lamella obtained by the subtraction of the CsCl-type layer is shown at the right panel.

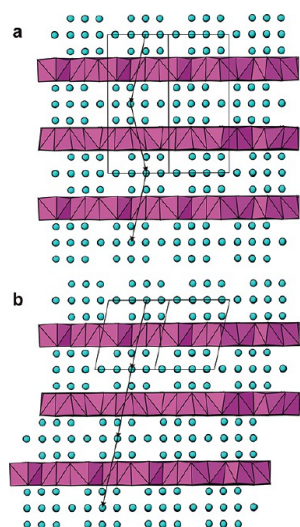**Figure 8.** Two possibilities of ordered displacement of the $Nd_{11}(SeO_3)_{12}$ blocks. Top: alternating displacements by $1/8[110]$ and $-1/8[110]$ projected vectors resulting in an orthorhombic structure. Bottom: cumulative displacement by a $1/8[110]$ projected vector only, resulting in a monoclinic structure (bottom right ED pattern in Figure 9).

Figure 9. $[1\bar{1}0]$ HRTEM images showing displacements of the $Nd_{11}(SeO_3)_{12}$ blocks. Top: alternating displacement over the $1/4[110]$ and $-1/4[110]$ projected vectors violated by the $1/8[110]$ displacement (marked with an arrowhead). Bottom: cumulative displacement by a $1/8[110]$ projected vector violated by the $-1/8[110]$ displacement (marked with an arrowhead).

antiprisms can be outlined. This ordering can be coupled with the Ln−Se−O−Cl block stacking causing differences in the largest lattice parameter. It seems that numerous stacking configurations of the $Nd_{11}(SeO_3)_{12}$ lamellas are possible in the $M_7Ln_{11}(SeO_3)_{12}Cl_{16}$ compounds because of the small energy difference between configurations caused by lateral displacements of these lamellas. It can be suggested that the $M_7Ln_{11}(SeO_3)_{12}Cl_{16}$ family presents order−disorder (OD) structures, as introduced by Dornberger-Schiff.[24]

Thus, many polytypes could be expected, but at the same time, large stacking disorder can be expected for these structures, causing difficulties in the preparation of single crystals suitable for structure refinement. This could be a reason for the apparent problem with the structure determination of the orthorhombic *Pban* phase with the lattice parameters $a = 15.941(1)$ Å, $b = 15.954(1)$ Å, and $c = 51.656(4)$ Å. It should
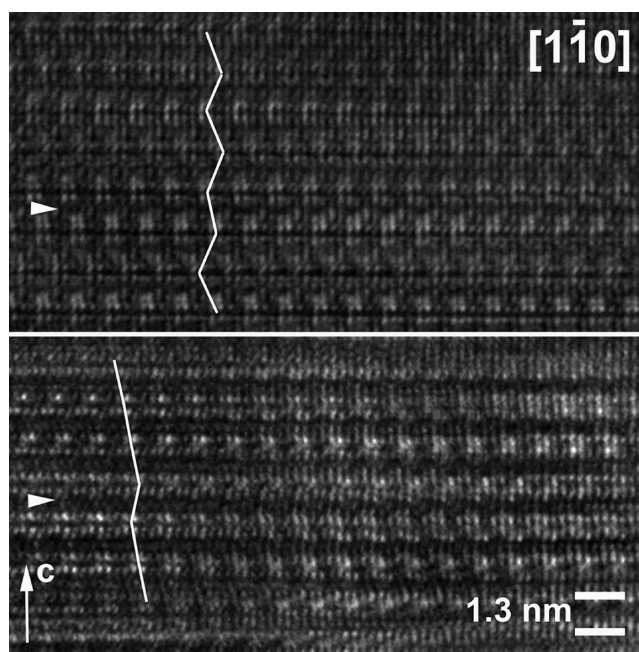
be noted that, although the observed ED patterns of this phase do not demonstrate noticeable diffuse intensity, stacking disorder cannot be excluded in this compound.

The compound is characterized by a bluish-pink body color, typical for materials with considerable neodymium content, caused by the many possible transitions within the $4f^3$ electronic configuration of Nd^{3+} lying in the visible part of the spectrum. The Nd^{3+} ion is known to show luminescence emission in the near-IR region in many compounds because of transitions from the $^4F_{3/2}$ multiplet to the ^4I_J multiplets, with $J = ^9/_2, ^{11}/_2, ^{13}/_2$, and $^{15}/_2$, yielding emissions at typically 0.90, 1.05, 1.35, and 1.85 μm, respectively. For most luminescent

Table 2. Composition and Unit Cell Constants for Known $M_xLn_{11}(SeO_3)_{12}Cl_y$ Selenite Chlorides

|			cell constant, Å			
compd no.	composition	space group	a	b	c	ref
1	$K_7Sm_{11}(SeO_3)_{12}Cl_{16}$	Pnan	15.6334	15.6640	25.0754	14
2	$Cs_7Pr_{11}(SeO_3)_{12}Cl_{16}$	Cmca	51.698	15.9990	15.9860	14
3	$Cs_7Nd_{11}(SeO_3)_{12}Cl_{16}$	Pna2$_1$	15.911	15.951	25.860	present study
4	$Cs_7Nd_{11}(SeO_3)_{12}Cl_{16}$	Pban	15.941	15.954	51.656	present study
5	$Rb_6LiPr_{11}(SeO_3)_{12}Cl_{16}$	I4/mcm	15.9058		24.7897	13
6	$Rb_6LiNd_{11}(SeO_3)_{12}Cl_{16}$	I4/mcm	15.8169		24.7702	9
7	$CaNd_{10}(SeO_3)_{12}Cl_8$	Ccca	15.588	17.419	15.681	23
8	$SrNd_{10}(SeO_3)_{12}Cl_8$	Ccca	15.773	17.622	15.836	23
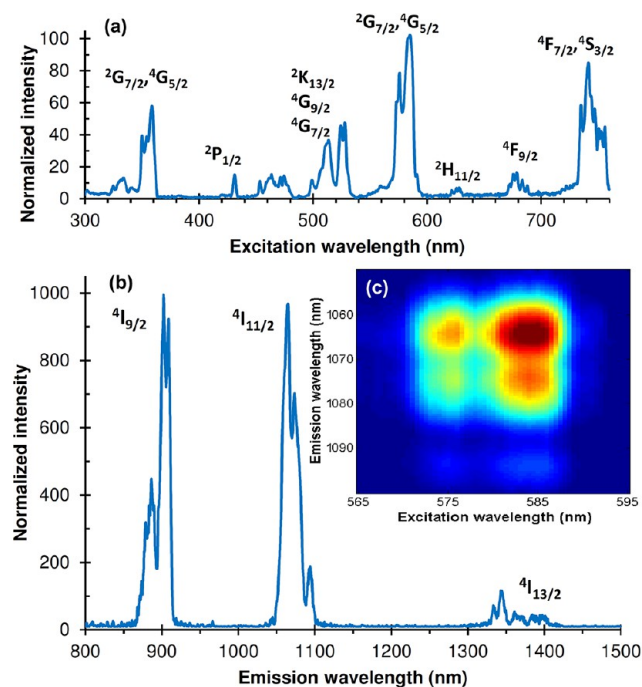
Figure 10. (a) Excitation spectrum at 75 K for the emission monitored at 1065 nm. (b) Emission spectrum at 75 K upon excitation at 584 nm. (c) Emission excitation map at 75 K for the ($^2G_{7/2}$, $^4G_{5/2}$) to $^4I_{11/2}$ transitions.

materials, the luminescence efficiency decreases for higher concentrations of the dopant ions because of nonradiative cross-relaxation. In this stoichiometric compound, this is also the case, and the emission intensity is relatively low. Nevertheless, detailed emission and excitation spectra could be obtained (Figure 10). The emission barycenters for the transitions from the $^4F_{3/2}$ multiplet to the $^4I_{9/2}$, $^4I_{11/2}$, and $^4I_{13/2}$ multiplets lie at 11143, 9348, and 7359 cm^{-1}, respectively, with an almost equal branching ratio for the transition to $^4I_{9/2}$ and $^4I_{11/2}$. Each multiplet shows a clear substructure, which is related to the crystal-field-induced splitting of each manifold. At room temperature, the spectra are very similar. To better resolve the emission bands, the spectra were also recorded at 75 K. As mentioned above, there are three clearly different coordination types in this compound for the 11 independent neodymium ions. Six have a 10-fold oxygen coordination (Nd1, Nd3, Nd5, Nd8, Nd9, and Nd10), one has an 8-fold oxygen coordination (Nd7), and four have a mixed coordination formed by four oxygen and four chlorine ions (Nd2, Nd4, Nd6, and Nd11). In principle, these three local environments give rise to a different splitting of the manifolds. This characteristic

has been repeatedly used as a probe for the local neighborhood of the neodymium ions.[25,26] However, in excitation−emission spectroscopy (inset of Figure 10), no variations of the emission spectrum as a function of the excitation wavelength are observed. Although the line widths of the individual transitions are relatively broad, which is to be expected for the high neodymium concentration in the compound, it appears that only one coordination is effectively contributing to the emission. For the neodymium exclusively coordinated by oxygen ions, there are eight or nine other neodymium ions within a distance of 6 Å, of which four to six ions are within 4.2 Å. Consequently, the probability of nonradiative cross-relaxation processes is very high. For (O, Cl) coordination of Nd2, Nd4, Nd6, and Nd11, there are only four other neodymium ions in the immediate vicinity (<6 Å). Therefore, it seems a reasonable hypothesis to assign the luminescence emission to the neodymium ions with mixed coordination. A similar dependence of the luminescence efficiency on the Nd−Nd distance was observed in neodymium phosphates.[27] Further support for the statement that only one type of coordination is contributing to the luminescence can be found in the substructure of the manifold at 1065 nm. The splitting of the $^4F_{3/2}$ multiplet (into two levels) and the $^4I_{11/2}$ (into six levels) gives rise to at most 12 distinct transitions, which is compatible with the observed emission spectrum (Figure S1 in the SI). However, the remaining uncertainty about the number of contributing neodymium ions to the luminescence, in combination with the considerably broadened emission lines, does not allow us to make stronger statements at present. Dedicated research is required to further link the luminescence and structural properties, but this is beyond the scope of this work.

4. CONCLUSIONS

During the spontaneous crystallization process, the NC $Cs_7Nd_{11}(SeO_3)_{12}Cl_{16}$ compound has been obtained in the NdOCl−CsCl−SeO$_2$ system. The crystal structure of $Cs_7Nd_{11}(SeO_3)_{12}Cl_{16}$ is represented as a stacking of the $Nd_{11}(SeO_3)_{12}$ lamellas with CsCl-like layers. The main difference between the $Cs_7Nd_{11}(SeO_3)_{12}Cl_{16}$ crystal structure and the other $M_7Ln_{11}(SeO_3)_{12}Cl_{16}$ compounds is the ordered arrangement of the neodymium atoms and vacancies in the $[NdO_4Cl_4]$ antiprisms. $Cs_7Nd_{11}(SeO_3)_{12}Cl_{16}$ demonstrates luminescence emission in the near-IR region with reduced efficiency due to a high concentration of the Nd^{3+} ions causing nonradiative cross-relaxation.

■ ASSOCIATED CONTENT

Ⓢ Supporting Information

CIF files with the crystal structure data, tables of atomic coordinates and equivalent isotropic temperature factors, emission spectrum for the transition recorded at 75 K, and the results for a pseudosymmetry search. This material is available free of charge via the Internet at http://pubs.acs.org.

■ AUTHOR INFORMATION

Corresponding Author

*E-mail: berdonosov@inorg.chem.msu.ru. Tel.: +7(495)939-3504. Fax: +7(495)939-0998.

Notes

The authors declare no competing financial interest.

■ REFERENCES

(1) Wickleder, M. S. *Chem. Rev.* **2002**, *102*, 2011−2087.

(2) Berdonosov, P. S.; Stefanovitch, S. Yu.; Dolgikh, V. A. *J. Solid State Chem.* **2000**, *149*, 236−241.

(3) Wickleder, M. S. *Acta Crystallogr.* **2003**, *E59*, i31−i32.

(4) Wickleder, M. S. *Z. Naturforsch.* **2002**, *57b*, 1414−1418.

(5) Berdonosov, P. S.; Shabalin, D. G.; Olenev, A. V.; Demianets, L. N.; Dolgikh, V. A.; Popovkin, B. A. *J. Solid State Chem.* **2003**, *174*, 111−115.

(6) Shabalin, D. G.; Berdonosov, P. S.; Dolgikh, V. A.; Oppermann, H.; Schmidt, P.; Popovkin, B. A. *Russ. Chem. Bull.* **2003**, *52*, 98−102.

(7) Ruck, M.; Schmidt, P. *Z. Anorg. Allg. Chem.* **2003**, *629*, 2133−2143.

(8) Wontcheu, J.; Schleid, Th. *J. Solid State Chem.* **2003**, *171*, 429−433.

(9) Lipp, C.; Schleid, Th. *Z. Kristallogr.* **2005**, No. Suppl. 22, 165.

(10) Lipp, C.; Schleid, Th. *Z. Anorg. Allg. Chem.* **2006**, *632*, 2150.

(11) Lipp, C.; Schleid, Th. *Z. Kristallogr.* **2006**, No. Suppl. 24, 171.

(12) Schleid, Th.; Wontcheu, J. *J. Alloys Compd.* **2006**, *418*, 45−52.

(13) Lipp, C.; Schleid, Th. *Z. Anorg. Allg. Chem.* **2006**, *632*, 2226−2231.

(14) Berdonosov, P. S.; Dolgikh, V. A.; Schmidt, P.; Ruck, M. Complex chloride−selenites of rare earthes—a family of new phases. IVth National Crystal Chemical Conference, Chernogolovka, Russia, June 26−30, 2006; Book of Abstracts; pp 192−193

(15) Berdonosov, P. S.; Oleneva, O. S.; Dolgikh, V. A. *Acta Crystallogr.* **2006**, *E62*, i29−i31.

(16) Brown, I. D. *Acta Crystallogr.* **1992**, *B48*, 553−572.

(17) Mo, X.; Hwu, Sh.-J. *Inorg. Chem.* **2003**, *42*, 3978−3980.

(18) Halasyamani, P. S. In *Functional Oxides*; Bruce, D. W., O'Hare, D., Walton, R. I., Eds.; Wiley: New York, 2010; pp 2−39.

(19) Akselrud, L. G.; Zavalii, P. Y.; Grin, Yu. N.; Pecharsky, V. K.; Baumgartner, B.; Wölfel, E. *Mater. Sci. Forum* **1993**, *133−136*, 335−342.

(20) Kurtz, S. K.; Perry, T. T. *J. Appl. Phys.* **1968**, *39*, 3798−3813.

(21) Morris, R. E.; Hriljac, J. A.; Cheetham, A. K. *Acta Crystallogr.* **1990**, *C46*, 2013−2017.

(22) Capillas, C.; Tasci, E. S.; de la Flor, G.; Orobengoa, D.; Perez-Mato, J. M.; Aroyo, M. I. *Z. Kristallogr.* **2011**, *226* (2), 186−196.

(23) Berdonosov, P. S.; Olenev, A. V.; Dolgikh, V. A.; Lightfoot, P. *J. Solid State Chem.* **2007**, *180*, 3019−3025.

(24) Dornberger-Schiff, K. *Acta Crystallogr.* **1956**, *9*, 593−601.

(25) Andrade, L. H. C.; Li, M. S.; Guyot, Y.; Brenier, A.; Boulon, G. *J. Phys.: Condens. Matter* **2006**, *18*, 7883−7892.

(26) Guzik, M.; Tomaszewicz, E.; Guyot, Y.; Legendziewicz, J.; Boulon, G. *J. Mater. Chem.* **2012**, *22*, 14896−14906.

(27) Godlewska, P.; Bandrowski, S.; MacAlik, L.; Lisiecki, R.; Ryba-Romanowski, W.; Szczygieł, I.; Ropuszyńska-Robak, P.; Hanuza, J. *Opt. Mater.* **2012**, *34*, 1023−1028.